Research in Astron. Astrophys. **2009** Vol. **9** No. **8**, 921 – 932
http://www.raa-journal.org *http://www.iop.org/journals/raa*

***R**esearch in*
***A**stronomy and*
***A**strophysics*

Interaction between granulation and small-scale magnetic flux observed by *Hinode* *

Jun Zhang, Shu-Hong Yang and Chun-Lan Jin

Key Laboratory of Solar Activity, National Astronomical Observatories, Chinese Academy of Sciences, Beijing 100012, China; *zjun@ourstar.bao.ac.cn*

Received 2009 February 23; accepted 2009 May 2

Abstract With the polarimetric observations obtained by the Spectro-Polarimeter on board Hinode, we study the relationship between granular development and magnetic field evolution in the quiet Sun. Six typical cases are displayed to exhibit interaction between granules and magnetic elements, and we have obtained the following results. (1) A granule develops centrosymmetrically when no magnetic flux emerges within the granular cell. (2) A granule develops and splits noncentrosymmetrically while flux emerges at an outer part of the granular cell. (3) Magnetic flux emergence in a cluster of mixed polarities is detected at the position of a granule as soon as the granule breaks up. (4) A dipole emerges accompanied by the development of a granule, and the two elements of the dipole are rooted in the adjacent intergranular lanes and face each other across the granule. Advected by the horizontal granular motion, the positive element of the dipole then cancels with the pre-existing negative flux. (5) Flux cancellation also takes place between a positive element, which is advected by granular flow, and its surrounding negative flux. (6) While magnetic flux cancellation takes place in a granular cell, the granule shrinks and then disappears. (7) Horizontal magnetic fields are enhanced at the places where dipoles emerge and where opposite polarities cancel each other, but only the horizontal fields between the dipolar elements point in an orderly way from the positive elements to the negative ones. Our results reveal that granules and small-scale magnetic fluxes influence each other. Granular flow advects magnetic flux, and magnetic flux evolution suppresses granular development. There exist extremely large Doppler blue-shifts at the site of one canceling magnetic element. This phenomenon may be caused by the upward flow produced by magnetic reconnection below the photosphere.

Key words: Sun: granulation — Sun: magnetic fields — Sun: photosphere — techniques: polarimetric

1 INTRODUCTION

Both observations and simulations reveal that granules and small-scale magnetic elements are spread all over the quiet Sun. Granules are bright isolated elements surrounded by intergranular lanes. The mean size of granules, excluding the surrounding dark lanes, amounts to 1.1″ (Namba & Diemel 1969), or 1.35″ (Bray et al. 1984), while the mean cell size of the granular elements, including one-half of the surrounding dark lanes, is 1.94″ (Bray & Loughhead 1977), or 1.76″ (Roudier & Muller 1986). Frequently, the granules expand and split into smaller components that drift apart, and the fragments may grow and fragment, merge with others, or shrink and decompose.

∗ Supported by the National Natural Science Foundation of China.

Magnetic fields in the quiet Sun can be classified into three categories based on their locations and morphologies: network (Leighton et al. 1962), intranetwork (IN; Livingston & Harvey 1975) and ephemeral regions (Harvey & Martin 1973). The network elements are confined to the supergranular boundaries and the IN ones are located within the supergranular cells. The spatial distribution and time evolution of IN magnetic features are closely associated with solar granulation (Lin & Rimmele 1999). Small flux and size with rapid time changes make the IN field difficult to observe and characterize (Keller et al. 1994). However, much progress has been made in IN morphology dynamics and some quantitative aspects, such as flux distributions (Wang et al. 1995), lifetimes (Zhang et al. 1998a), mean horizontal velocity fields (Wang et al. 1996; Zhang et al. 1998b), motion patterns and evolution (Zhang et al. 1998b, c, 2006).

The magnetic flux emergence seems to be significantly influenced by granular motion. Research about horizontal IN fields suggests that small magnetic loops are being advected toward the surface by the convective upward motion of the plasma inside the granules (Lites et al. 1996; Orozco Suárez et al. 2008). The horizontal motion inside the granules carries the vertical magnetic flux toward the intergranular lanes (Harvey et al. 2007; Centeno et al. 2007). Then, most of these IN magnetic elements are destroyed by three mechanisms: merging with IN or network elements of the same polarity, cancelation of opposite polarity elements, or separation and disappearance at the position where they appear (Zhang et al. 1998a). Furthermore, the magnetic emergence also has an important influence on the shape of the underlying granulation pattern leading to the so-called "abnormal granulation" (Cheung et al. 2007).

Using the continuum intensities, vector magnetic fields and Doppler velocities derived from the Stokes profiles obtained by the Spectro-Polarimeter (SP; Lites et al. 2001) aboard Hinode (Kosugi et al. 2007), we mainly study the relationships between the development of granular structures and the emergence and cancelation of small-scale (with a typical size of $\sim 1''$ in this paper) magnetic elements from their birth to death. In Section 2, we describe the observations and the strategy of Stokes profile inversion. Then we present the relationships between granular development and magnetic flux emergence (in Sect. 3) and cancelation (in Sect. 4). The conclusions and discussion are given in Section 5.

2 OBSERVATIONS AND INVERSION STRATEGY

The SP instrument of the Solar Optical Telescope (SOT; Ichimoto et al. 2008; Shimizu et al. 2008; Suematsu et al. 2008; Tsuneta et al. 2008) aboard Hinode provides the full Stokes profiles of two Fe lines at 630.15 nm ($g_{\rm eff} = 1.67$) and 630.25 nm ($g_{\rm eff} = 2.5$) in four modes (fast map, dynamics, normal map and deep magnetogram). In order to investigate both the structure and the evolution of granules and magnetic elements, the observational field-of-view (FOV) should not be too small and the cadence should be high enough. Hence, we adopt the data taken from 11:33 UT to 17:51 UT on June 1, 2007 in the fast map mode. These data consist of 92 sets of SP maps with a 2-minute cadence, and the observational target is a quiet Sun region near the disk center ($-6''$, $-199''$) with a FOV of $8.86'' \times 162.3''$. The scan step (X direction in Fig. 1) is $0.295''$, and the pixel sampling along the slit direction (Y direction in Fig. 1) is $0.32''$. The integration time for each slit was 3.2 s with a noise level in the polarization continuum of $1.4 \times 10^{-3} I_c$.

By using the inversion techniques based on the assumption of a Miline−Eddington atmospheric model (Yokoyama 2008, in preparation), we can derive vector magnetic fields from the full Stokes profiles. Although the inversion procedures encounter difficulties in convergence toward and uniqueness of solutions when confronted with noisy profiles (Lites et al. 2008), they will be largely independent of the noise and the field strength initialization if only the pixels with polarization signals above a reasonable threshold are inverted (Orozco Suárez et al. 2007). Here, we only analyze the pixels with total polarization degrees above the noise level in the polarization continuum in order to exclude some profiles that cannot be inverted reliably.

Values of 13 free parameters are returned from the inversion, including the three components of magnetic field (field strength B, inclination angle γ, azimuth angle ϕ), the stray light fraction α, the Doppler velocity $V_{\rm los}$, and so on. Since the pair of Fe I lines in the low flux quiet Sun regions are not capable of distinguishing between the intrinsic magnetic field and the filling factor (Martínez González et

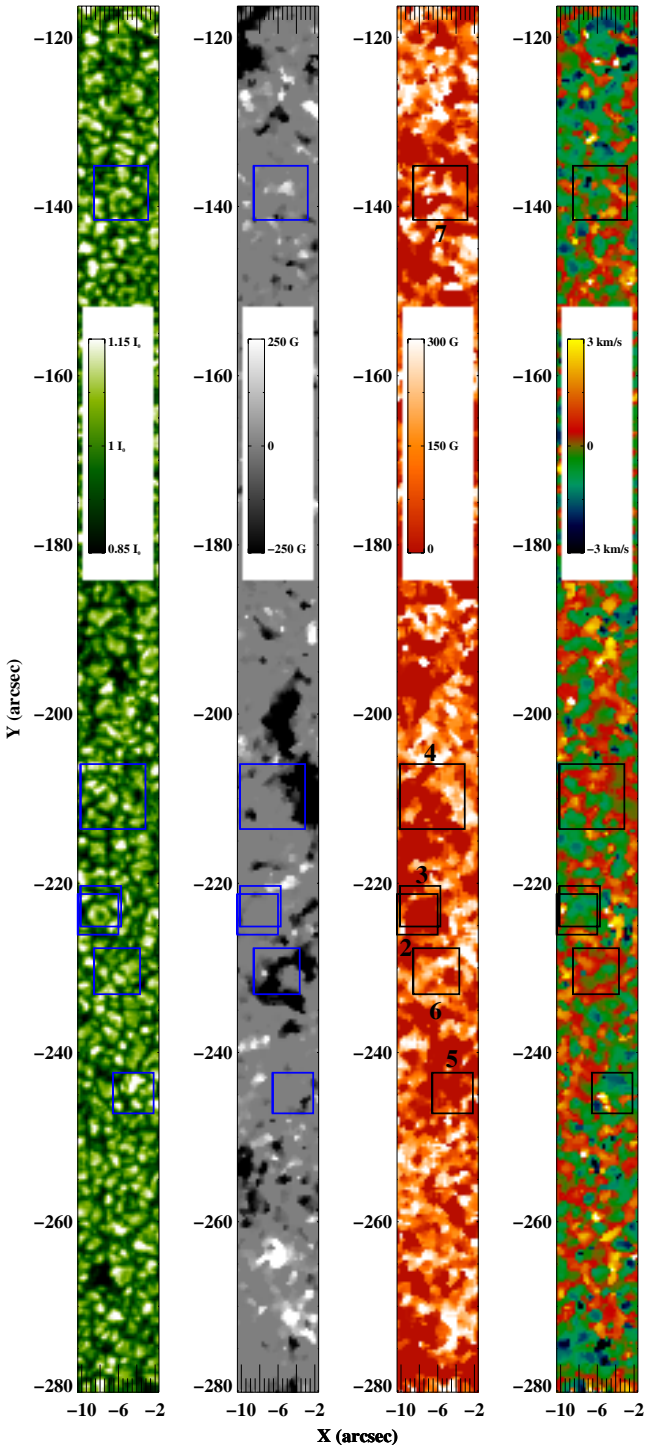

Fig. 1 General appearance of the whole field-of-view (FOV) retrieved from the SP data obtained from 14:29:54 UT to 14:31:51 UT on 2007 June 1. *From left to right*: continuum intensity map, corresponding longitudinal magnetogram, transverse magnetogram, and Dopplergram. Windows 2−7 outline the FOVs of Figs. 2 − 7, respectively. I_0 represents the average continuum intensity in the whole FOV.

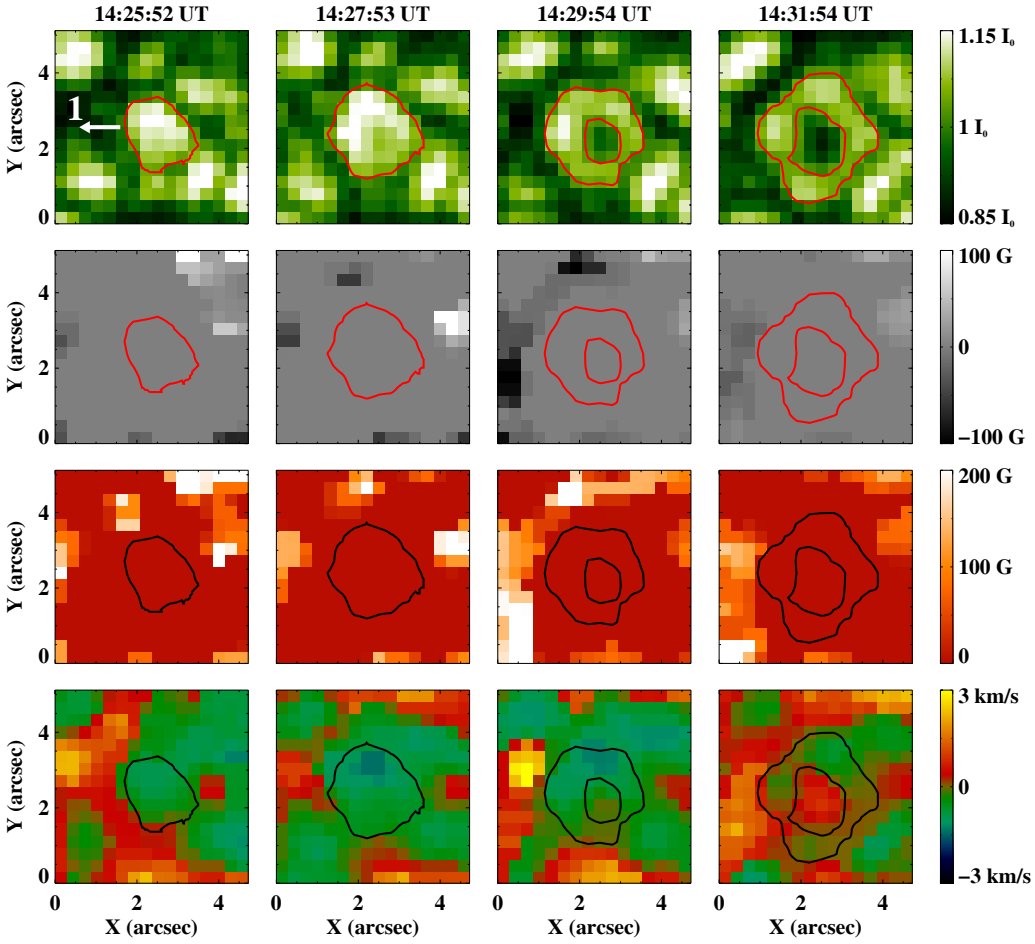

Fig. 2 Temporal evolution of a granule with no magnetic flux emergence. *From top to bottom*: continuum intensity, corresponding longitudinal field, transverse field and Doppler velocity. The contours in the top row panels represent the granule with continuum intensity $I_c/I_0 = 1.03$, and they are also overplotted on the corresponding magnetograms and Dopplergrams. Here, the only granule we focus on studying is selected by the outline. Arrow "1" denotes the direction of granular flow along which we calculate the apparent horizontal velocity.

al. 2006), the flux density is a more appropriate quantity to describe. Here, we show the equivalent, spatially resolved vector magnetic fields by "apparent flux density" of the longitudinal and transverse components (Lites et al. 1999), i.e. $B^L_{\rm app} = (1\text{-}\alpha)B\cos\gamma$ and $B^T_{\rm app} = (1\text{-}\alpha)^{1/2}B\sin\gamma$, respectively. The longitudinal component $B^L_{\rm app}$ may be considered as the magnitude of the line-of-sight (LOS) component of a spatially resolved magnetic field that produces the circular polarization signal as the observed signal, and the transverse component $B^T_{\rm app}$ is vertical to the LOS that would produce the observed linear polarization signal. In the vector field measurements based on the Zeeman Effect, there exists a 180 degree ambiguity in determining the field azimuth. Potential field approximation is one of the fairly acceptable methods to resolve the ambiguity (Wang 1999). The Doppler velocities, which are evaluated from the center of the Stokes I profiles according to the Fe 630.25 nm line and averaged over the whole FOV, are well defined even in weak field regions (Chae et al. 2004).

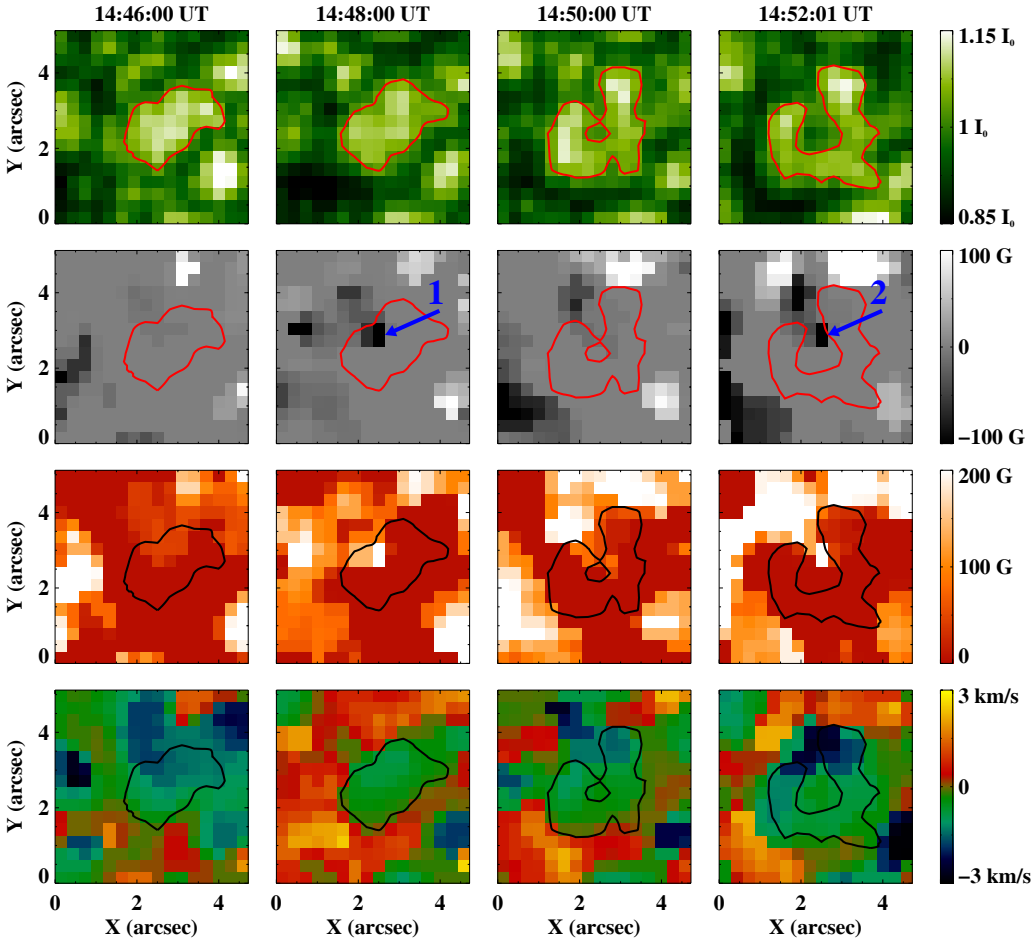

Fig. 3 Similar to Fig. 2 but for a granule which accompanies flux emergence. Arrows "1" and "2" denote two magnetic elements emerging in an orderly way at an outer part of the granule.

Figure 1 shows the whole FOV images retrieved from the SP data obtained from 14:29:54 UT to 14:31:51 UT. They include a continuum intensity map, the corresponding longitudinal magnetogram, transverse magnetogram, and Dopplergram from left to right, respectively. The zero value areas in the magnetograms represent the pixels not included in the analysis because of their low polarization signals. Windows 2−7 in Figure 1 outline the corresponding FOVs of Figures 2−7, respectively. Windows 4 and 6 are located near network magnetic fields, while others are at IN fields.

3 RELATIONSHIP BETWEEN GRANULAR DEVELOPMENT AND MAGNETIC FLUX EMERGENCE

In order to explore the relationship between granular development and magnetic flux emergence in the quiet Sun, we examine a time sequence of continuum intensity maps, corresponding vector magnetograms and Dopplergrams. We find that granules and magnetic elements influence each other in complicated ways. Here, we display several typical cases representing different interacting forms between them.

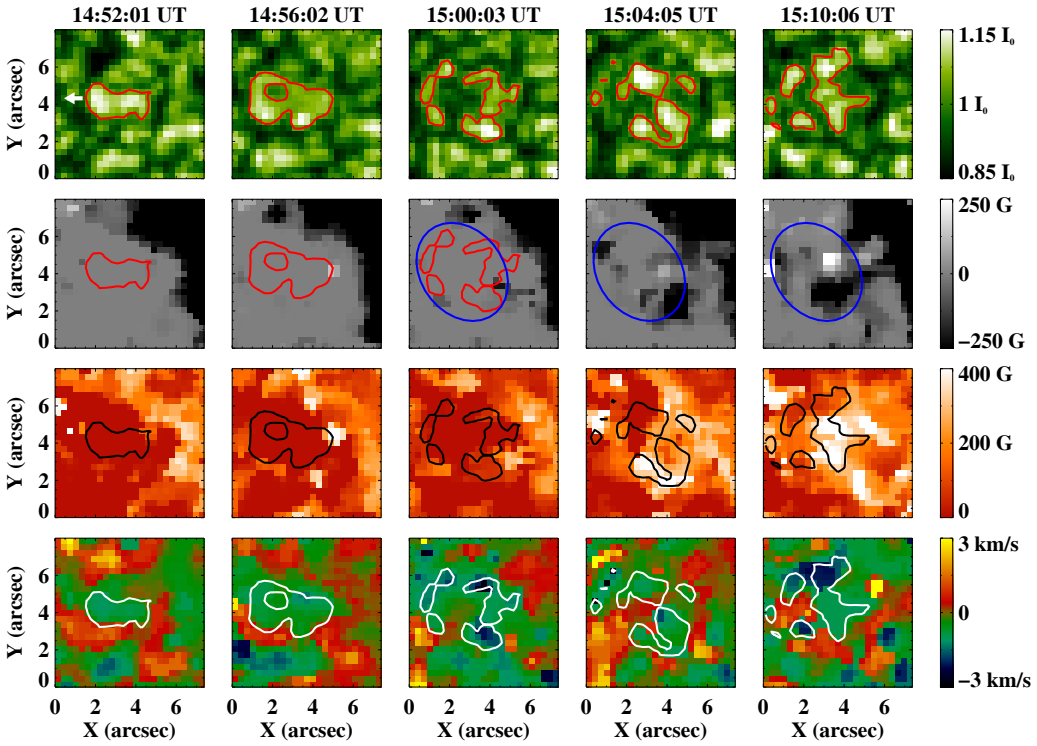

Fig. 4 Similar to Fig. 2 but for magnetic flux emergence as a cluster of mixed polarities following the split of a granule. The ellipses enclose the area where the flux emerges.

It appears that a granular structure develops centrosymmetrically when no magnetic flux emerges within the granular cell, just as shown in Figure 2. The contour curves outline the granule which we focused on studying with the continuum intensity ratio $I_c/I_0 = 1.03$, where I_0 represents the average continuum intensity in the whole FOV. From 14:25 UT on, the granule continuously expanded with a mean apparent horizontal velocity of 1.5 km s^{-1} (calculated along the direction of arrow "1"). At 14:29 UT, a dark core appeared near the granular center and expanded larger. Comparing the maps of continuum intensity with the Dopplergrams, we can see that the granular cells always suffered Doppler blue-shifts during their development process.

We have also noticed that a granular structure develops and splits noncentrosymmetrically while magnetic flux emerges within the granular cell. A typical example is exhibited in Figure 3. Arrows "1" and "2" denote two negative elements emerging in an orderly way at an outer part of the granule within 6 min, and their maximum longitudinal apparent flux density reached 100 Mx cm^{-2}. Different from the granular shape shown in Figure 2, the boundary of this granule became concave as the magnetic flux emerged. At 14:50 UT, the granule split into several small fragments.

Figure 4 shows that lots of magnetic elements emerged as a cluster of mixed polarities while a granule broke up. The granule first appeared at 14:46 UT, then developed gradually and became larger with a mean apparent horizontal expanding velocity of 1.6 km s^{-1} along the direction indicated by the arrow. The main body of the granule split at 15:00 UT; meanwhile the magnetic flux was detected emerging as a cluster of mixed polarities at the position that the initial granule was located (defined by the ellipses in the longitudinal magnetograms), and reached that its maximum absolute value of 4.2×10^{18} Mx at 15:10 UT.

Observations also indicate that the granular motion has a significant influence on the magnetic flux emergence. As shown in the first two columns of Figure 5, a dipole emerged accompanying the development of a granule. A pair of arrows labeled "2" denote the two magnetic elements of the dipole. At 16:12 UT, the positive element of the dipole appeared and the transverse fields had generally ordered directions (shown by thin arrows in the transverse magnetograms at 16:12 UT). At this time, the granular region suffered larger Doppler blue-shifts with a mean velocity of $-1.8\,\mathrm{km\ s^{-1}}$. Two minutes later, the other element of the dipole appeared and the transverse fields between the dipolar elements were enhanced with their directions pointing in an orderly way from the positive element to the negative one. The two elements of the dipole then lay on the two sides of the granule, rooted in the adjacent intergranular lanes.

4 RELATIONSHIP BETWEEN GRANULAR DEVELOPMENT AND MAGNETIC FLUX CANCELATION

Magnetic flux cancelation is a main form of flux disappearance in the solar photosphere, but its physical mechanism is not clearly known in detail. Because of lacking magnetic field observations with high temporo-spatial resolution, the behavior of flux cancelation at a sub-arcsec spatial scale has not been well researched.

The last three columns in Figure 5 exhibit the flux cancelation which occurred between the positive element of the dipole and pre-existing negative flux. The positive element (shown by arrow "3") was advected by the horizontal flow with a mean velocity of $1.7\,\mathrm{km\ s^{-1}}$ along the direction of arrow "1" towards the pre-existing negative element (denoted by arrow "4"). At 16:18 UT, they encountered each other and canceled violently; meanwhile strong transverse fields (see the square area) appeared, but their directions were unordered, i.e. with no consistency in orientation. By 16:20 UT, the positive element had disappeared completely.

Figure 6 displays a case of magnetic flux cancelation between a positive element (indicated by arrow "1") and its surrounding negative flux. During the growing and splitting process of a granule, the positive element was advected by the granular flow along the direction of arrow "2" with a mean velocity of $1.0\,\mathrm{km\ s^{-1}}$. At 16:08 UT, it encountered the negative network fields and canceled with them. Four minutes later, the positive element disappeared totally. Dopplergrams in this figure also show that the granular locations were occupied by the Doppler blue-shift signals.

Besides being advected by granular motion, canceling magnetic flux also suppresses granular development, as shown in Figure 7. With the growing process of a granule, a dipole began to emerge at 16:22 UT, and the horizontal magnetic fields between the dipolar elements also appeared, with their directions pointing from the positive element to the negative one, as shown by the arrows in the parallelogram's "II" region. This dipole was much more obvious at 16:24 UT (shown by a pair of arrows "2"). Before the appearance of dipole "2", there already existed another dipole (denoted by a pair of arrows "1"). From 16:20 UT to 16:26 UT, the pre-existing dipole moved to the newly emerged dipole, with an average velocity of $2.2\,\mathrm{km\ s^{-1}}$. The negative element of dipole "1" and the positive element of dipole "2" canceled since 16:24 UT. Two minutes later, the canceling negative element split into two segments (denoted by arrows "3" and "4", respectively), due to the collision of the canceling positive element (see arrow "5"). Then the positive element of dipole "1" began to move away from the canceling position along the direction of arrow "6" with an average velocity of $2.6\,\mathrm{km\ s^{-1}}$, and finally returned to its birth place. The negative element of the newly emerging dipole also moved away from the canceling position along the direction of arrow "7", with an average velocity of $2.5\,\mathrm{km\ s^{-1}}$. At 16:28 UT, segment "3" had disappeared, while segment "4" and element "5" were canceling violently. At this time, strong transverse fields (inside the parallelogram's "III" region) appeared at the canceling position, but their directions were unordered. At 16:30 UT, the two canceling elements almost disappeared. From the continuum intensity maps, we can clearly see that the granule shrank rapidly while the magnetic flux cancelation took place. Comparing the longitudinal magnetograms with the corresponding Dopplergrams, we find that, at 16:26 UT, the site of dipolar element "5" (outlined by the ellipses) underwent very high Doppler velocity ($-3.0\,\mathrm{km\ s^{-1}}$).

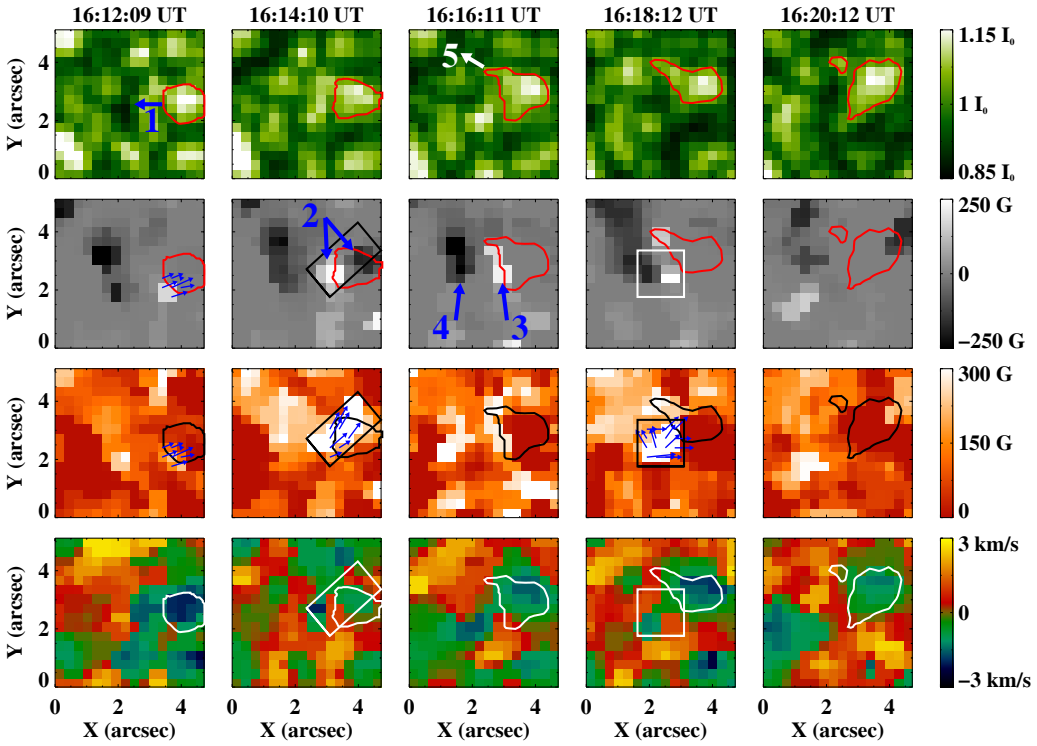

Fig. 5 Similar to Fig. 2 but for emergence of a dipole (first two columns; marked by a pair of arrows "2") and cancelation (last three columns) between a positive element (indicated by arrow "3") belonging to the dipole and a pre-existing negative element (shown with arrow "4"). The parallelograms and squares embody the regions where the transverse fields are enhanced, and the thin arrows indicate the directions of the local horizontal fields. Arrow "1" denotes the direction along which we calculate the apparent horizontal velocity of the granular flow and arrow "5" the direction along which the granule quickly extended.

5 CONCLUSIONS AND DISCUSSION

By examining six typical cases in this paper, we present the relationship between emerging (canceling) small-scale magnetic flux and granular structures in a quiet Sun region near the disk center. A granule develops in a centrosymmetric form under the condition that no magnetic flux emerges within the granular cell, and another granular structure develops and splits in a noncentrosymmetrical form while flux emerges at an outer part of the granular cell. As soon as a granule breaks up, magnetic flux emerges as a cluster of mixed polarities appears at the position of the former granule. A dipole emerges accompanying the development of a granule and cancels pre-existing flux, due to the advection of the horizontal granular motion. When magnetic flux cancelation takes place at a granular position, the granule shrinks and disappears. Our results confirm the idea that granular flow advects magnetic flux and magnetic flux evolution suppresses granular development. Furthermore, we uncover the evolution of transverse fields and changes in Doppler signals during the canceling process.

Observations show that the horizontal fields of small magnetic loops are advected toward the surface by the upward motion of the plasma inside the granules (Lites et al. 1996) and horizontal motion inside the granules carries the vertical magnetic flux toward the intergranular lanes (Harvey et al. 2007; Centeno et al. 2007). In this paper, the emergence of the dipole connected by horizontal fields which

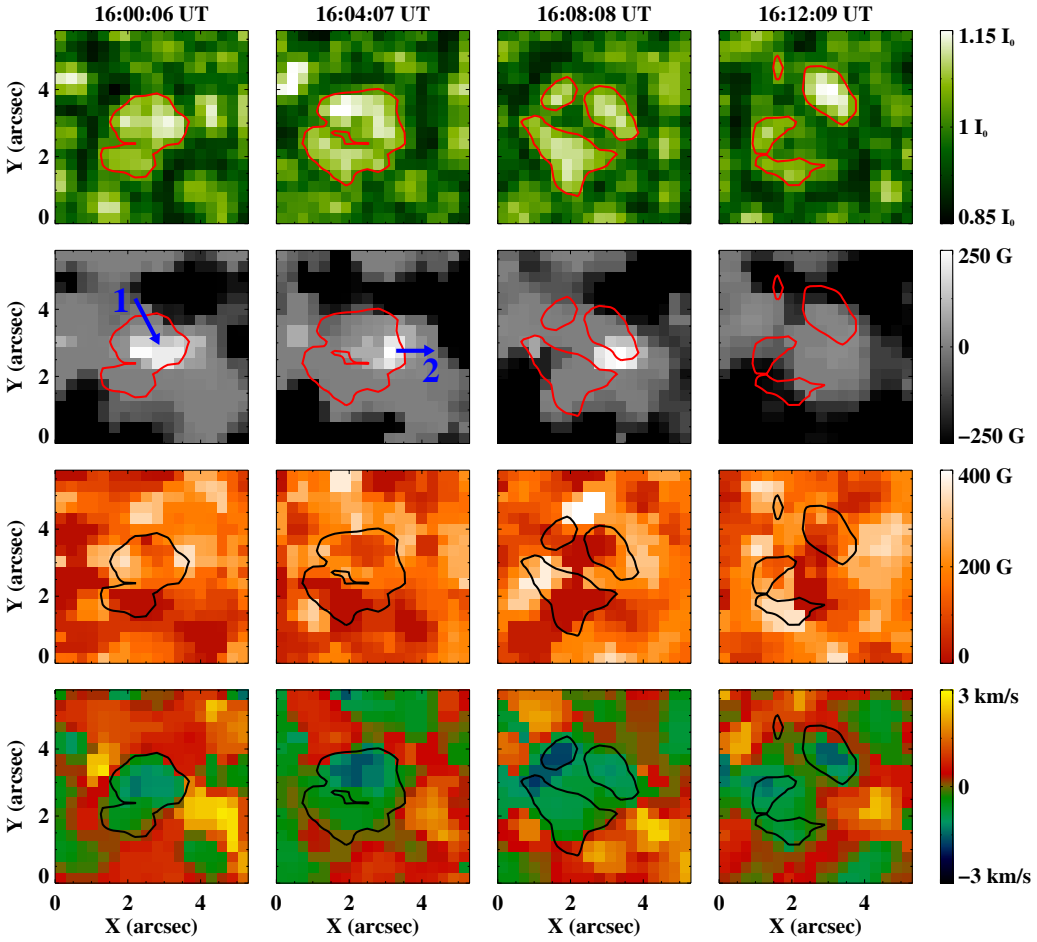

Fig. 6 Similar to Fig. 2 but for flux cancelation of a positive element advected by the granular flow with its surrounding negative flux. Arrow "1" denotes the positive element and arrow "2" direction of movement for the element.

pointed from the positive element to the negative one, as shown in Figure 5, is another case similar to that of Centeno et al. (2007). However, we cannot exclude the possibility that the two elements of dipole "2" spontaneously separated from each other without the driving effect of the granular plasma motion when they emerged continuously in an Ω-shaped configuration. Figure 4 shows that magnetic flux emerged as a cluster of mixed polarities at a position where the granule was located and was detected as soon as the granule split. The split of the granule may result from the emergence of the magnetic flux. There also exists another possibility that the granule split without affecting its surroundings, and then the flux emerged upward by magnetic buoyancy or by convection. In a simulation, Cheung et al. (2007) found that the magnetic flux emergence with a longitudinal flux of more than 10^{19} Mx disturbs the granulation, while small-scale flux tubes with less than 10^{18} Mx are not sufficiently buoyant to rise coherently against the granulation and produce no visible disturbance in the granules. Our results in this observational study are inconsistent with Cheung et al. (2007), since the emerging magnetic elements with flux lower than 10^{18} Mx, e.g. the event displayed in Figure 3, can also affect granular development.

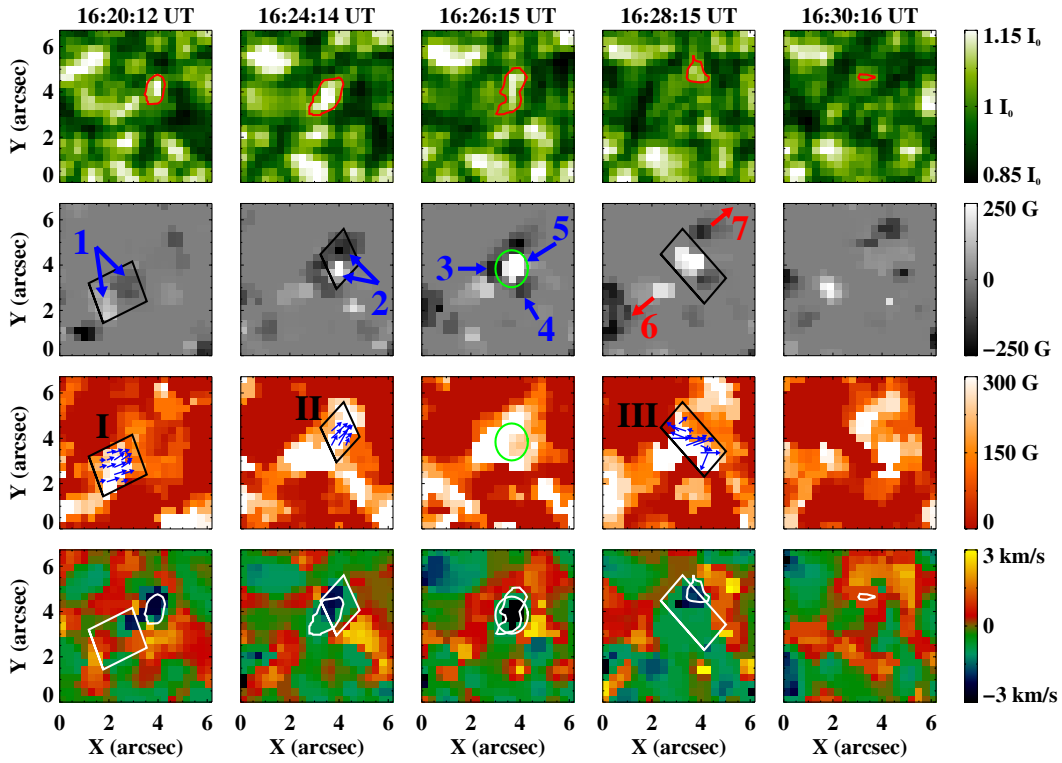

Fig. 7 Similar to Fig. 2 but for the shrinking process of a granule due to the cancelation between the positive element of a dipole (shown by a pair of arrows "2") and the negative element of another dipole (denoted by another pair of arrows "1"). Arrows "3" and "4" indicate two segments dividing from the negative element of dipole "1", and arrow "5" shows the positive element of dipole "2". Arrows "6" and "7" denote the directions of movement for the non-interacting elements of the two dipoles. The parallelograms and the thin arrows within them are the same as described in Fig. 5. Note that the arrows in parallelogram's "II" are overplotted from the transverse fields at the same location at 16:22 UT. The ellipses mark the position where the remarkable Doppler blue-shifts are located.

Two of the six cases indicate that magnetic cancelation was triggered by the pushing effect of the horizontal granular flows (see Figs. 5 and 6). On the other hand, the magnetic element also reacted to granules. The example in Figure 5 reveals that the development of the granule was suppressed by the positive element (denoted by arrow "3"). At 16:20 UT, the element disappeared; meanwhile, the granule occupied the element position. Vector magnetic field observations show that the magnetic connection of canceling elements was changed, and the transverse fields were enhanced during the canceling process (see Figs. 5 and 7). These observations confirm the earlier results that the two components of canceling magnetic features are initially not connected by transverse fields above the photosphere (Zhang et al. 2001). These results are also consistent with Kubo & Shimizu (2007), who examined several collision events and found the formation of new magnetic connections.

Granules are upward-moving, hot parcels of gas, exhibiting blue-shifts in the high-resolution spectral image (Nesis et al. 2001). Not unexpectedly in this study, granules always suffered Doppler blue-shifts with an average velocity of $-1.1\,\mathrm{km\ s^{-1}}$. In Figure 5, the maximum Doppler blue-shift was $-2.0\,\mathrm{km\ s^{-1}}$ at the early emerging stage of dipole "2", while it decreased to $-0.9\,\mathrm{km\ s^{-1}}$ when the dipole was well developed. In Figure 7, the region with Doppler blue-shifts of about $-3.0\,\mathrm{km\ s^{-1}}$ at 16:26 UT is coincident with the site of the canceling magnetic element "5", which belonged to the

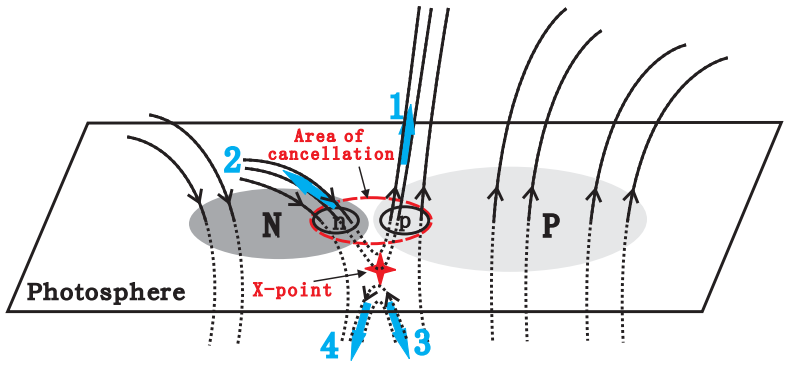

Fig. 8 Sketch illustrating the formation of large Doppler blue-shifts located at one of the canceling magnetic elements. See the text for details.

newly emerging dipole "2". At the early emerging stage (at 16:20 UT) of this dipole, when the Doppler blue-shifts are expected to be the largest during the dipolar lifetime, the Doppler velocity is around $-2.2\,\mathrm{km\,s^{-1}}$, smaller than that at the canceling stage. We suggest that the excess of blue-shifts at 16:20 in Figure 7 is produced by the magnetic flux reconnection below the photosphere, as demonstrated in Figure 8. When magnetic reconnection occurs at the so-called "X-point", magnetic energy is converted into thermal energy and kinetic energy. Then, bi-directional plasma jets are formed and ejected from the "X-point" along the field lines. If the reconnection takes place below the photosphere, the upward plasma jets (denoted by arrows "1" and "2") move across the solar surface from the inner region to the outer one, and Doppler blue-shifts will be observed in the photospheric surface. The area where the larger blue-shifts appear is relevant to the topology of magnetic field lines. The magnetic field lines that jet "1" moves along are more vertical than those of jet "2", so the blue-shifts appear at the site of one magnetic element (marked by "p"). Chae et al. (2004) reported an example of magnetic flux submergence at the flux canceling sites. Their observations also revealed that larger downflows were at the canceling positive magnetic feature instead of at the polarity inversion line. If magnetic fields are observed with lower spatial resolution, small-scale elements cannot be distinguished separately and several elements combine together to form a larger one. Under this condition, the large blue-shifts will appear mainly at the adjacent region of the two big canceling elements (marked by "N" and "P" in Fig. 8). However, we cannot rule out the possibility that the large upward velocities in the cancelation area are caused by the emerging U−shaped flux loops (Parker 1984; Lites et al. 1995).

Since this study is limited to only several cases, we will make a statistical analysis over a large sample of events to examine whether these results are general or not in our next study.

Acknowledgements We thank the *Hinode* team for providing the data. *Hinode* is a Japanese mission developed and launched by ISAS/JAXA, with NAOJ as a domestic partner and NASA and STFC (UK) as international partners. It is operated by these agencies in co-operation with ESA and NSC (Norway). This work is supported by the National Natural Science Foundations of China (Nos. 10573025, 40674081 and 40890161), the CAS Project KJCX2-YW-T04, and the National Basic Research Program of China under grant G2006CB806303.

References

Bray, R. J., & Loughhead, R. E. 1977, Sol. Phys., 54, 319
Bray, R. J., Loughhead, R. E., & Durrant, C. J. 1984, The solar granulation (2nd ed.; Cambridge and New York: Cambridge University Press), 270
Centeno, R., Socas-Navarro, H., Lites, B., et al. 2007, ApJ, 666, L137
Chae, J., Moon, Y., & Pevtsov, A. A. 2004, ApJ, 602, L65
Cheung, M. C. M., Schüssler, M., & Moreno-Insertis, F. 2007, A&A, 467, 703
Harvey, K. L., & Martin, S. F. 1973, Sol. Phys., 32, 389
Harvey, J. W., Branston, D., Henney, C. J., & Keller, C. U. 2007, ApJ, 659, 177
Ichimoto, K., Lites, B., Elmore, D., et al. 2008, Sol. Phys., 249, 233
Keller, C. U., Deubner, F. L., Egger, U., et al. 1994, A&A, 286, 626
Kosugi, T., Matsuzaki, K., Sakao, T., et al. 2007, Sol. Phys., 243, 3
Kubo, M., & Shimizu, T. 2007, ApJ, 671, 990
Leighton, R. B., Noyes, R. W., & Simon, G. W. 1962, ApJ, 135, 474
Lin, H., & Rimmele, T. 1999, ApJ, 514, 448
Lites, B. W., Elmore, D. F., & Streander, K. V. 2001, in ASP Conf. Series, 236, 33
Lites, B. W., Kubo, M., Socas-Navarroet, H. et al. 2008, ApJ, 672, 1237
Lites, B. W., Leka, K. D., Skumanich, A., et al. 1996, ApJ, 460, 1019
Lites, B. W., Low, B. C., Martinez Pillet, V., et al. 1995, ApJ, 446, 877
Lites, B. W., Rutten, R. J., & Berger, T. E. 1999, ApJ, 517, 1013
Livingston, W. C., & Harvey, J. 1975, BAAS, 7, 346
Martínez González, M. J., Collados, M., & Ruiz Cobo, B. 2006, A&A, 456, 1159
Namba, O., & Diemel, W. E. 1969, Sol. Phys., 7, 167
Nesis, A., Hammer, R., & Roth, M. 2001, Sol. Phys., 200, 11
Orozco Suárez, D., Bellot Rubio, L. R., Del Toro Iniesta, J. C., et al. 2007, PASJ, 59, 837
Orozco Suárez, D., Bellot Rubio, L. R., Del Toro Iniesta, J. C., & Tsuneta, S. 2008, A&A, 481, L33
Parker, E. N. 1984, ApJ, 280, 423
Roudier, T., & Muller, R. 1986, Sol. Phys., 107, 11
Shimizu, T., Nagata, S., Tsuneta, S., et al. 2008, Sol. Phys., 249, 221
Suematsu, Y., Tsuneta, S., Ichimoto, K., et al. 2008, Sol. Phys., 249, 197
Tsuneta, S., Ichimoto, K., Katsukawa, Y., et al. 2008, Sol. Phys., 249, 167
Wang, H., Tang, F., Zirin, H., & Wang, J. 1996, Sol. Phys., 165, 223
Wang, J. 1999, Fundam. Cosmic Phys., 20, 251
Wang, J., Wang, H., Tang, F., et al. 1995, Sol. Phys., 160, 277
Zhang, J., Lin, G., Wang, J., et al. 1998a, Sol. Phys., 178, 245
Zhang, J., Lin, G., Wang, J., Wang, H., & Zirin, H. 1998c, A&A, 338, 322
Zhang, J., Ma, J., & Wang, H. 2006, ApJ, 649, 464
Zhang, J., Wang, J., Deng, Y., & Wu, D. 2001, ApJ, 548, L99
Zhang, J., Wang, J., Wang, H., & Zirin, H. 1998b, A&A, 335, 341